Joint Beamforming and Association Design for MIMO Radar

Urs Niesen and Jayakrishnan Unnikrishnan

Abstract

A critical task of a radar receiver is data association, which assigns radar target detections to target filter tracks. Motivated by its importance, this paper introduces the problem of jointly designing multiple-input multiple-output (MIMO) radar transmit beam patterns and the corresponding data association schemes. We show that the coupling of the beamforming and the association subproblems can be conveniently parameterized by what we term an ambiguity graph, which prescribes if two targets are to be disambiguated by the beamforming design or by the data association scheme. The choice of ambiguity graph determines which of the two subproblems is more difficult and therefore allows to trade performance of one versus the other, resulting in a detection-association trade-off. This paper shows how to design both the beam pattern and the association scheme for a given ambiguity graph. It then discusses how to choose an ambiguity graph achieving close to the optimal detection-association trade-off.

I. Introduction

A. Motivation and Summary of Results

One of the key advantages of multiple-input multiple-output (MIMO) radar systems is that they enable adaptive transmit beamforming. This technique adaptively steers radar beams to better illuminate a target of interest while reducing the received signal contribution from other targets, jammers, or clutter [2]. There has been significant recent interest in designing these transmit beam patterns, summarized in Section I-B below.

The performance of a transmit beam pattern depends on the corresponding receiver architecture. A standard radar receiver architecture for tracking targets consists of two main building blocks: detection of potential targets and track filtering (see, e.g., [3, Chapter 7.3.4], [4], [5]). The two are linked by an association step, which uses the target priors to assign each detection to one of the tracks. The association step ensures that all the detections assigned to the same track are in fact caused by a single target across time. Correct association is critical, since errors in this step can lead to tracking failure.

The simplest transmit beamforming methods focus on optimizing coverage within the field of view. More advanced methods utilize prior information from the tracker, such as estimates of the targets' azimuth angles. However, to the best of our knowledge, prior work effectively ignores the association step during the beamforming design (see Section I-B).

In this paper, we initiate the joint design of the beam pattern and the data association scheme. We show that the coupling of the two is captured by what we term an *ambiguity graph*. The vertices of this graph are the targets. Two vertices connected by an edge correspond to targets that are "difficult" to disambiguate using the prior distributions during data association. They therefore should not be simultaneously illuminated by the beam pattern. Conversely, two vertices not connected by an edge correspond to targets that are "easy" to disambiguate during data association. They therefore do not place any constraints on the beam pattern. The choice of precisely which targets are "difficult" or "easy" to disambiguate allows to trade the performance of the beamformer and the association scheme. We refer to this as the *detection-association trade-off*.

The joint beamforming and association design problem can then be broken up into three subproblems: First, designing an optimal beam pattern respecting the constraints of a given ambiguity graph. Second,

finding an appropriate association scheme for a beam pattern with the given ambiguity graph. Third, choosing a Pareto-optimal ambiguity graph operating on the boundary of the detection-association trade-off.

We term the first subproblem the *ambiguity-aware beamforming* problem. We show that the ambiguity-aware beamforming problem can be formulated as a semidefinite optimization problem, which is efficiently solvable using interior-point methods. Through analysis and several simulations, we demonstrate two types of performance improvements due to the beamforming being ambiguity aware: an improvement in *transmit power gain* and an improvement in *target identifiability*. The transmit power gain increases detection performance for a fixed number of targets. The improvement in target identifiability increases the number of targets that can be tracked for a fixed number of radar antennas. Through analysis and numerical simulations, we demonstrate that both of these gains can be quite substantial.

To solve the second subproblem, we propose an *ambiguity-aware nearest-neighbor* association scheme. This association scheme is a generalization of the well-known nearest-neighbor association scheme. Unlike that scheme, it explicitly takes the structure of the beam pattern (captured by the ambiguity graph) into account. The proposed association scheme has a cubic worst-case computational complexity in the number of targets being tracked.

Finally, we consider the third subproblem of choosing a Pareto-optimal ambiguity graph operating on the boundary of the detection-association trade-off. This problem turns out to be a computationally difficult combinatorial optimization problem. We therefore propose a design heuristic and show through simulations that it can yield near-optimal performance.

B. Related Work

Multi-antenna radar systems can broadly be classified into two categories: phased arrays [3, Chapter 3], in which phase-shifted versions of the same signal are emitted from the antennas, and MIMO radar [2], in which general signals can be emitted from the antennas. The increased adaptability of MIMO radar offers significant advantages over phased-array radar, including increased target identifiability and flexibility in transmit beam pattern design [2].

A number of prior works have studied the problem of designing transmit beam patterns for MIMO radar systems. These methods vary in the amount of prior target information, generally obtained from the track filters at the receiver, they utilize. Some methods do not use any prior target information and focus on creating beam patterns with wide coverage [6].

A large body of literature creates beam patterns adapted to the tracked targets' azimuth angles. One such approach designs the beam pattern using a two-step process, which first selects a cross-correlation matrix to achieve a desired beam pattern and then chooses signals having that correlation [7]. Another approach decouples the spatial and temporal dimensions of the beamforming design [8], [9]. Yet another class of methods adopts a beam-space approach to beamformer design [10]–[14], which aims to combine the benefits of phased-array and MIMO radar. Beamformer designs that are robust to mismatches between the presumed and actual beamforming vectors are studied in [15]. In the automotive context, beamforming has also been studied from the perspective of interference avoidance [16].

A few recent works [17], [18] have addressed the question of adapting beam patterns for improved detection. Some works focus on adapting waveforms to account for change in clutter in the radar scene [19]–[21], while other works focus on adaptive beamforming to improve tracking [17], [22], [23].

The different methods described above design beamforming patterns to maximize detection accuracy and are not directly concerned with the resulting association problem. In contrast, in this paper we explicitly take the data association problem into account while designing the beam pattern, and we show that there is in fact a trade-off between the detection and the association performance.

C. Organization

The remainder of this paper is organized as follows. Section II introduces the problem setting. Section III shows how to solve the ambiguity-aware beamforming problem. Ambiguity-aware association schemes

and how to choose a Pareto-optimal ambiguity graph are discussed in Section IV. Section V contains discussions and concluding remarks.

II. PROBLEM SETTING

We consider a monostatic radar system with N antennas. Denote by $a_n^*(\theta) \in \mathbb{C}$ and $b_n(\theta) \in \mathbb{C}$ the transmit and receive gains of antenna n at azimuth angle θ. Assume we emit the complex, baseband-equivalent, vector-valued signal $\boldsymbol{s}(t) \in \mathbb{C}^N$ with $t \in [0, T)$ from the antenna array. The corresponding (noiseless, baseband-equivalent) received signal after reflection from a point target with unit radar cross-section at range $\tau c/2$, Doppler shift ω, and azimuth angle θ is

$$\boldsymbol{x}(t; \tau, \omega, \theta) \triangleq \boldsymbol{b}(\theta)\boldsymbol{a}^\dagger(\theta)\boldsymbol{s}(t - \tau)\exp(j\omega t).$$

Note that here and in the following we use lowercase bold font for vectors and uppercase bold font for matrices. The vector $\boldsymbol{a}(\theta)$ has components $a_n(\theta)$ and similar for the vector $\boldsymbol{b}(\theta)$. The symbol $\cdot^\dagger$ denotes the conjugate transpose. Finally, c denotes the speed of light. For general radar cross-section $h \in \mathbb{C}$, the reflected signal is $h\boldsymbol{x}(t; \tau, \omega, \theta)$. Observe that the radar cross-section h includes the path loss.

For K targets with parameters $(\tau_k, \omega_k, \theta_k)$ and radar cross-section h_k for $k \in \{1, 2, \ldots, K\}$, the received signal is then

$$\boldsymbol{y}(t) \triangleq \sum_{k=1}^{K} h_k \boldsymbol{x}(t; \tau_k, \omega_k, \theta_k) + \boldsymbol{z}(t),$$

where $\boldsymbol{z}(t)$ is Gaussian receiver noise.

We aim to track the parameters of these K targets from the received signal $\boldsymbol{y}(t)$. The standard receiver architecture uses a matched filter bank, with each filter tuned to one parameter triple. The output of the matched filter tuned to (τ, ω, θ) is

$$
\begin{aligned}
r(\tau, \omega, \theta) &\triangleq \sum_{n=1}^{N} \int_{t=\tau}^{T+\tau} y_n(t)x_n^*(t; \tau, \omega, \theta)\, dt \\
&= \sum_{n=1}^{N} \int_{t=\tau}^{T+\tau} y_n(t)\boldsymbol{s}^\dagger(t - \tau)\exp(-j\omega t)\, dt\, \boldsymbol{a}(\theta)b_n^*(\theta).
\end{aligned}
\tag{1}
$$

Following [8], we make throughout the remainder of this paper the assumption that the transmitted signal has the form

$$\boldsymbol{s}(t) \triangleq \boldsymbol{W}\tilde{\boldsymbol{s}}(t)$$

for some matrix $\boldsymbol{W} \in \mathbb{C}^{N \times N}$ satisfying $\text{tr}(\boldsymbol{W}\boldsymbol{W}^\dagger) = 1$ and for some $\tilde{\boldsymbol{s}}(t) \in \mathbb{C}^N$ with support $t \in [0, T)$ and with approximate bandwidth B. Here, $\tilde{\boldsymbol{s}}(t)$ is assumed to have good cross-correlation properties, meaning that it has matrix-valued ambiguity function $\boldsymbol{\chi}(\Delta\tau, \Delta\omega) \in \mathbb{C}^{N \times N}$ satisfying

$$
\begin{aligned}
\boldsymbol{\chi}(\Delta\tau, \Delta\omega) &\triangleq \int_{t=\max\{\Delta\tau, 0\}}^{T+\min\{\Delta\tau, 0\}} \tilde{\boldsymbol{s}}(t)\tilde{\boldsymbol{s}}^\dagger(t - \Delta\tau)\exp(-j\Delta\omega t)\, dt \\
&\approx 1_{(0,0)}(\Delta\tau, \Delta\omega)\boldsymbol{I},
\end{aligned}
\tag{2}
$$

where

$$1_{(0,0)}(\Delta\tau, \Delta\omega) \triangleq \begin{cases} 1, & \text{if } (\Delta\tau, \Delta\omega) = (0, 0), \\ 0, & \text{otherwise.} \end{cases}$$

The temporal support T and the bandwidth B of the waveforms place limits of order $1/B$ on the resolution of $\Delta\tau$ and of order $1/T$ on the resolution of $\Delta\omega$. The identity (2) holds up to those resolution limits. See Appendix A for a formal definition of these limits. In the same appendix, we also describe and analyze a construction for waveforms having property (2) for large enough values of time-bandwidth product BT.

For simplicity, we make in the remainder of the paper the assumption that (2) holds with equality, i.e., that the ambiguity function is ideal.

Assuming an ideal ambiguity function, the matched filter output (1) can be simplified after some algebra to

$$r(\tau, \omega, \theta) = \sum_{k=1}^{K} h_k \exp\big(-j(\omega - \omega_k)\tau_k\big) 1_{(0,0)}(\tau - \tau_k, \omega - \omega_k) \boldsymbol{b}^\dagger(\theta)\boldsymbol{b}(\theta_k)\boldsymbol{a}^\dagger(\theta_k)\boldsymbol{R}\boldsymbol{a}(\theta) + \tilde{z}(\tau, \omega, \theta), \quad (3)$$

where

$$\boldsymbol{R} \triangleq \boldsymbol{W}\boldsymbol{W}^\dagger$$

is the *beamforming matrix* and $\tilde{z}(\tau, \omega, \theta)$ is the filtered receiver noise. Observe that $\boldsymbol{R}$ satisfies $\mathrm{tr}(\boldsymbol{R}) = \mathrm{tr}(\boldsymbol{W}\boldsymbol{W}^\dagger) = 1$.

A common procedure for tracking the parameters $(\tau_k, \omega_k, \theta_k)$ for the K targets consists of two steps, a *detection* step followed by an *association* step. In the first step, we detect the targets. This is done by thresholding the matched filter outputs $r(\tau, \omega, \theta)$. I.e., we find all $(\hat{\tau}, \hat{\omega}, \hat{\theta})$ such that $|r(\hat{\tau}, \hat{\omega}, \hat{\theta})|$ is strictly above some threshold. In the second step, we associate each such detection $(\hat{\tau}, \hat{\omega}, \hat{\theta})$ with a target track using an association rule.

Assume that we have prior information about the parameters $(\tau_k, \omega_k, \theta_k)$. This prior is typically derived from the output of the prediction stage of a filter tracking these targets. It can be used to define a *gate*, i.e., a region of parameter space in which we expect the true parameters for a fixed target to fall. Similar to other works in the literature [8], we make for now the simplifying assumption that the prior information on the azimuth angle is precise, so that θ_k is in effect known a priori. Section V discusses how this assumption can be relaxed. With this assumption, the gate $\mathcal{S}_k$ for target k is a subset of $\mathbb{R}^2$ in which we expect the parameter tuple (τ_k, ω_k) to fall.

We now formalize a somewhat stylized association rule that we will use throughout the paper: For each target track $k \in \{1, 2, \ldots, K\}$, find all detections of the form $(\hat{\tau}, \hat{\omega}, \hat{\theta})$ with $(\hat{\tau}, \hat{\omega}) \in \mathcal{S}_k$, and $\hat{\theta} = \theta_k$ (which is known a priori by assumption). If there is a single such detection, then we associate it with the track for target k. If there are zero or more than one such detections, then we declare an association error. In this association rule, the priors are used to gate the detections. Further, the detection-to-track association is performed only if this gating removes all association ambiguity. While this association rule is quite simple, it includes several standard rules as special cases.

Example 1 (Rectangular Gates)**.** From the prior, we can derive lower bounds (τ_k^-, ω_k^-) and upper bounds (τ_k^+, ω_k^+) for the parameter tuple (τ_k, ω_k). For example, τ_k^+ could be chosen as the prior mean of τ_k plus three standard deviations (and similarly for the other bounds). We can then construct the standard rectangular gating set $\mathcal{S}_k \triangleq [\tau_k^-, \tau_k^+] \times [\omega_k^-, \omega_k^+]$. $\diamondsuit$

Example 2 (Nearest-Neighbor Gates)**.** Let $f_k(\tau, \omega)$ be the prior density on the parameters (τ_k, ω_k) of target k. Set

$$\mathcal{S}_k \triangleq \big\{(\tau, \omega) : f_k(\tau, \omega) > f_{k'}(\tau, \omega) \text{ for all } k' \neq k\big\}.$$

See Fig. 1 for an illustration. The resulting gating sets partition the space $\mathbb{R}^2$. For Gaussian priors with equal variance, the resulting partition is a Voronoi partition. The corresponding association rule assigns each detection to the track it most likely came from. This is similar to the standard nearest-neighbor or greedy association rule. $\diamondsuit$

For future reference, we define

$$\mathcal{E}_k \triangleq \big\{k' \in \{1, 2, \ldots, K\} \setminus \{k\} : \mathcal{S}_{k'} \cap \mathcal{S}_k \neq \emptyset\big\} \quad (4)$$

as the targets k' that are a-priori ambiguous with respect to target k.
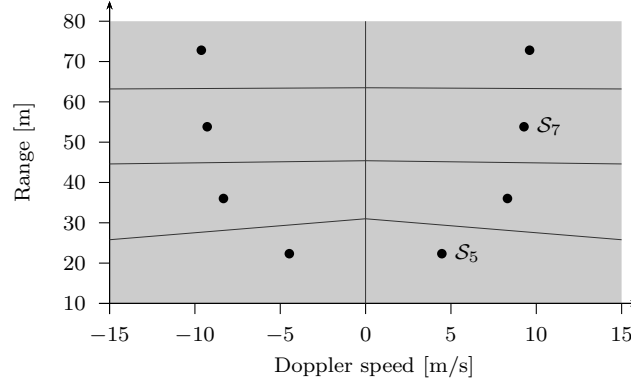
Fig. 1. Illustration of nearest-neighbor gating sets $\{\mathcal{S}_k\}$. The dots show the expected target parameters from the priors. The figure assumes equal-variance Gaussian priors, so that the resulting gating sets form a Voronoi partition.

To understand the interaction between data association and beamforming, consider initially a scenario with $K = 2$ targets with known azimuth angles θ_1 and θ_2. Assume the matched filter outputs $|r(\tau_1, \omega_1, \theta_1)|$, $|r(\tau_1, \omega_1, \theta_2)|$, $|r(\tau_2, \omega_2, \theta_1)|$, $|r(\tau_2, \omega_2, \theta_2)|$ are all above the detection threshold. Without further knowledge we cannot unambiguously solve the association problem. Indeed, (τ_1, ω_1) could be correctly associated with target one and (τ_2, ω_2) correctly with target two. However, alternatively, (τ_1, ω_1) could be incorrectly associated with target two and (τ_2, ω_2) incorrectly with target one. Without additional information, both associations are equally valid from the radar receiver's point of view.

This ambiguity can be resolved in two ways. First, through additional prior information about τ_k and ω_k. If the gates $\mathcal{S}_1$ and $\mathcal{S}_2$ do not intersect (or, equivalently, if $2 \notin \mathcal{E}_1$), then one of the two data associations is invalidated by the prior.

Second, by designing the transmitted signals to ensure that two of the matched filter outputs are less than the detection threshold, say δ. I.e.,

$$|r(\tau_1, \omega_1, \theta_2)| \leq \delta,$$
$$|r(\tau_2, \omega_2, \theta_1)| \leq \delta.$$

In this case, one of the two data associations is invalidated by the observations.

Consider next the general case with K targets. Assume for the moment that the received signal is noiseless, and set the detection threshold to zero. Under this assumption and using (3), the matched filter output $r(\hat{\tau}, \hat{\omega}, \hat{\theta})$ is nonzero, and hence a potential target detected, if and only if $(\hat{\tau}, \hat{\omega}) = (\tau_k, \omega_k)$ for some $k \in \{1, 2, \ldots, K\}$ satisfying

$$|h_k \boldsymbol{b}^\dagger(\hat{\theta}) \boldsymbol{b}(\theta_k) \boldsymbol{a}^\dagger(\theta_k) \boldsymbol{R} a(\hat{\theta})| \neq 0.$$

Consider the resulting association problem. Our association rule (defined just above Example 1) will assign all detections to tracks without declaring an error if, for every k, there is exactly one tuple $(\hat{\tau}, \hat{\omega})$ inside the gating set $\mathcal{S}_k$ for target k such that $r(\hat{\tau}, \hat{\omega}, \theta_k)$ is nonzero.

From the above discussion, the association problem has a unique solution if the following two sufficient conditions hold. First, for every $k \in \{1, 2, \ldots, K\}$,

$$|h_k| \|\boldsymbol{b}(\theta_k)\|^2 \boldsymbol{a}^\dagger(\theta_k) \boldsymbol{R} a(\theta_k) > 0,$$

so that the correct target is detected. Second, for every $k \in \{1, 2, \ldots, K\}$ and every $k' \in \mathcal{E}_k$,

$$h_k \boldsymbol{b}^\dagger(\theta_{k'}) \boldsymbol{b}(\theta_k) \boldsymbol{a}^\dagger(\theta_k) \boldsymbol{R} a(\theta_{k'}) = 0,$$

so that hard to disambiguate targets are not simultaneously illuminated. This second condition ensures that the association is unambiguous. Crucially, these conditions depend solely on the prior knowledge of the target parameters (i.e., the gates $\mathcal{S}_k$ and the azimuths θ_k).

To focus on the essential aspect of the problem, we enforce in the following the slightly stronger condition that

$$\boldsymbol{a}^\dagger(\theta_k)\boldsymbol{R}\boldsymbol{a}(\theta_k) > 0, \tag{5}$$

for every k and that

$$\boldsymbol{a}^\dagger(\theta_k)\boldsymbol{R}\boldsymbol{a}(\theta_{k'}) = 0 \tag{6}$$

for every k and $k' \in \mathcal{E}_k$.

To guard against receiver noise, we further want the transmit power gaing (5) to be as large as possible for all targets. In fact, for fixed detection threshold, we can upper bound the probability of detection error as a decreasing function of the left-hand side of (5) for the worst target k (see, e.g., [3, Chapter 6.3]). The optimal *ambiguity-aware beamforming problem* is therefore[1]

$$
\begin{aligned}
&\underset{\boldsymbol{R} \in \mathbb{C}^{N \times N}}{\text{maximize}} \quad \underset{k \in \{1,2,\dots,K\}}{\min} \boldsymbol{a}^\dagger(\theta_k)\boldsymbol{R}\boldsymbol{a}(\theta_k) \\
&\text{subject to} \quad \boldsymbol{a}^\dagger(\theta_k)\boldsymbol{R}\boldsymbol{a}(\theta_{k'}) = 0, \quad \forall k \text{ and } \forall k' \in \mathcal{E}_k, \\
&\qquad\qquad\qquad\qquad \text{tr}(\boldsymbol{R}) = 1, \\
&\qquad\qquad\qquad\qquad\quad \boldsymbol{R} \succeq 0
\end{aligned} \tag{7}
$$

Here $\boldsymbol{R} \succeq 0$ denotes that the matrix $\boldsymbol{R}$ is positive semidefinite (which implies that it is Hermitian).

The structure of the ambiguity-aware beamforming problem can be conveniently described by a graph with vertices $\{1, 2, \dots, K\}$ (one for each target) and an edge between vertex k and k' if $k' \in \mathcal{E}_k$. Since $k' \in \mathcal{E}_k$ if and only if $k \in \mathcal{E}_{k'}$ by construction, this graph is undirected. We refer to this graph as the *ambiguity graph* in the following. The next example introduces a special case of this graph that will be used to illustrate the results throughout the paper.

Example 3 (Ambiguity Graph). Consider a vehicular scenario with a radar at a crossroad on which several cars are driving in the same direction. This scenario is depicted in Fig. 2(a). The corresponding expected values of the target parameters τ_k and ω_k are shown in Fig. 2(b) by black dots together with rectangular gates $\mathcal{S}_k \triangleq [\tau_k^-, \tau_k^+] \times [\omega_k^-, \omega_k^+]$ as defined in Example 1 indicated in gray. Observe from Fig. 2(b) that only the gating sets of neighboring vehicles intersect. The resulting ambiguity graph is depicted in Fig. 2(c). ◇

Remark 1: If we have no prior information about the parameters τ_k and ω_k, then all targets are a-priori ambiguous. The resulting ambiguity graph is therefore complete (i.e., has and edge between every pair of distinct targets). In this case, the ambiguity-aware beamforming problem essentially reduces to the setting in [8]. However, for partial ambiguity graphs, like the one introduced in Example 3, the problem and its solution are quite different. This connection is discussed further in Example 7 in Section III.

III. OPTIMAL AMBIGUITY-AWARE BEAMFORMING

The ambiguity-aware beamforming problem defined in (7) can be solved efficiently as follows. Note that the function $\boldsymbol{a}^\dagger(\theta_k)\boldsymbol{R}\boldsymbol{a}(\theta_k)$ is linear in $\boldsymbol{R}$ and hence, in particular, concave. Since the minimum of concave functions is again concave, this implies that the objective function of (7) is concave in $\boldsymbol{R}$. The conditions $\boldsymbol{a}^\dagger(\theta_k)\boldsymbol{R}\boldsymbol{a}(\theta_{k'}) = 0$ and $\text{tr}(\boldsymbol{R}) = 1$ are linear in $\boldsymbol{R}$. Further, we have the positive semidefiniteness constraint $\boldsymbol{R} \succeq 0$, which describes a convex set. Thus, we are dealing with a convex problem, which can actually be rewritten as a semidefinite program by introducing a slack variable to handle the minimization over k. These programs can be solved efficiently using interior-point methods [24].

We illustrate this approach with several examples.

---

[1]To minimize the aforementioned probability of detection error, the term $|h_k|\|\boldsymbol{b}(\theta_k)\|^2$ should be added to the objective function of (7). We prefer to drop this term here to simplify the notation, since it does not change the nature of the problem as discussed above. Further, the hard zero-forcing constraint (6) could be replaced by a weaker constraint that the interfering signal contribution is below the noise floor, as is discussed in Section V.
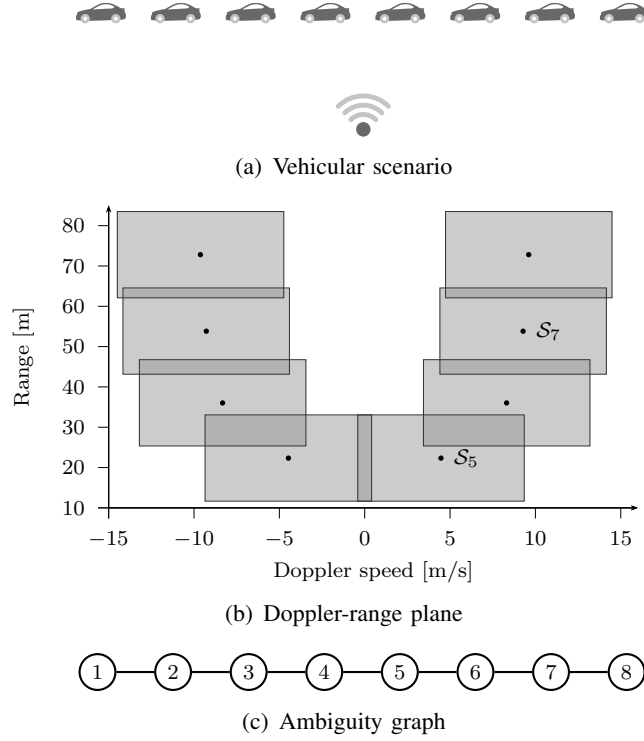
(a) Vehicular scenario

(b) Doppler-range plane

(c) Ambiguity graph

Fig. 2. Vehicular scenario, resulting parameter ambiguity in the Doppler-range plane, and corresponding ambiguity graph.

Example 4. Consider a scenario with $N = 3$ uniformly spaced antennas at half-wavelength separation and with $K = 3$ targets at azimuth angles $\theta_1 = -60°$, $\theta_2 = 0°$, and $\theta_3 = 60°$. The corresponding transmit antenna gains are

$$a_n(\theta) \triangleq \exp\big(j(n-1)\pi \sin(\theta)\big). \tag{8}$$

Assume first that the ambiguity graph is complete (i.e., $\mathcal{E}_k \triangleq \{1, 2, \ldots, K\} \setminus \{k\}$ for each k so that the ambiguity graph has an edge between every pair of targets). The corresponding optimal transmit beam pattern $\boldsymbol{a}^\dagger(\theta_k)\boldsymbol{R}\boldsymbol{a}(\theta)$ with $\boldsymbol{R}$ the solution to (7) as a function of azimuth angle θ for fixed θ_k is shown in red/gray in Fig. 3.

Assume next that the ambiguity graph contains only edges between neighboring targets (as introduced in Example 3). The corresponding optimal transmit beam pattern is shown in black in Fig. 3.

Comparing the two curves in Fig. 3, two key differences are apparent. First, the beam pattern for the complete ambiguity graph has an additional null in Figs. 3(a) and 3(c). Second, by not having to enforce these nulls, the beam pattern for the partial ambiguity graph is able to increase the transmit power gain at the desired target by $4.3\,\mathrm{dB}$ (from $-3.2\,\mathrm{dB}$ to $1.1\,\mathrm{dB}$). $\diamondsuit$

As the previous example shows, taking the reduced ambiguity between the targets (captured by the ambiguity graph being incomplete) into account can improve the transmit power gain. This improvement is explored further in the next example.

Example 5 (Transmit Power Gain)**.** Consider N uniformly spaced antennas at half-wavelength separation and with $K = N$ targets. Target $k \in \{1, 2, \ldots, K\}$ has azimuth angle $\theta_k \triangleq \big((2k-1)/K - 1\big)90°$. In words, the targets are uniformly spaced in azimuth. For $N = K = 3$, this reduces to the setting in Example 4.

We compare the optimal beamforming matrices designed according to (7) for a complete ambiguity graph and for a partially connected graph with edges only between neighboring targets k and $k+1$ for all $k \in \{1, 2, \ldots, K-1\}$ (see again Example 3). The transmit power gain ratio, i.e., the ratio of the quantity $\min_{k \in \{1,2,\ldots,K\}} \boldsymbol{a}^\dagger(\theta_k)\boldsymbol{R}\boldsymbol{a}(\theta_k)$ between the two scenarios is shown in Fig. 4 as a function of the number

(a) $|\boldsymbol{a}^{\dagger}(\theta_1)\boldsymbol{R}\boldsymbol{a}(\theta)|$

(b) $|\boldsymbol{a}^{\dagger}(\theta_2)\boldsymbol{R}\boldsymbol{a}(\theta)|$

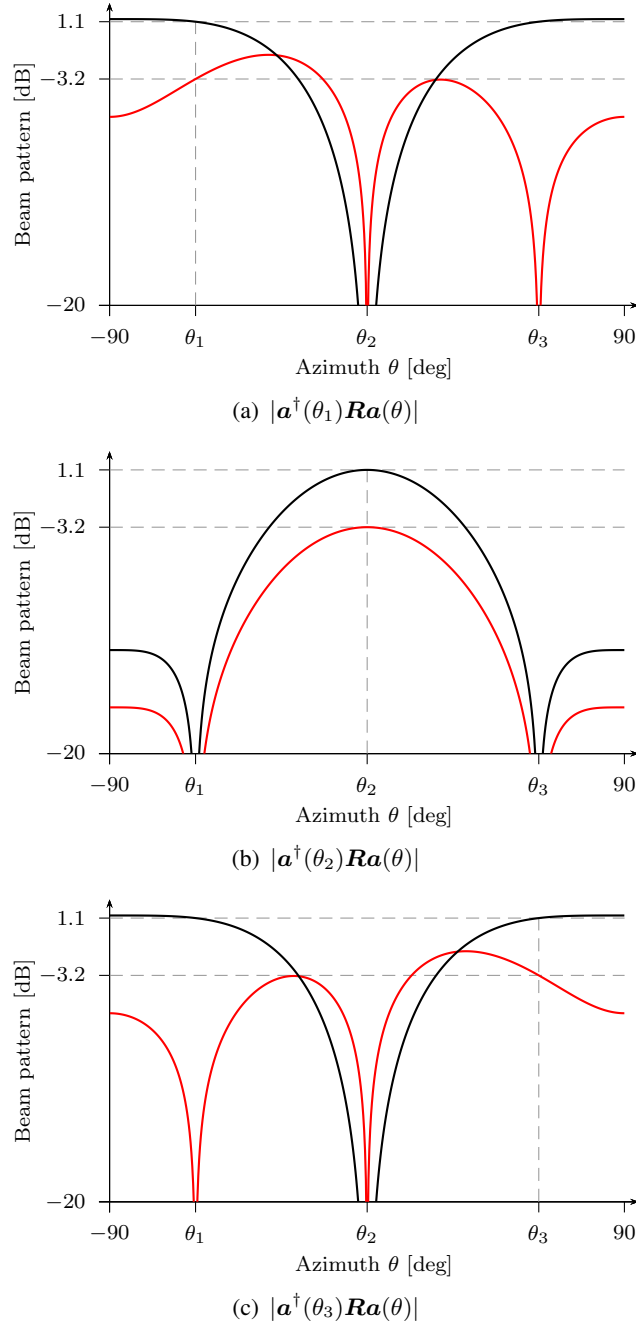(c) $|\boldsymbol{a}^{\dagger}(\theta_3)\boldsymbol{R}\boldsymbol{a}(\theta)|$

Fig. 3. Optimal transmit beam patterns for two scenarios with $N = 3$ antennas and $K = 3$ targets. The red/gray curve (–) is for the scenario of complete ambiguity. The black curve (–) is for the scenario of ambiguity only between neighbors (i.e., not between θ_1 and θ_3).

of transmit antennas N. As is clear from the figure, explicitly taking the target ambiguity into account can yield a significant improvement in transmit power gain that increases with the problem size. ◇

The last example indicates that ambiguity-aware beamforming can substantially improve the transmit power gain. In other words, for the same number of targets, we can expect better detection performance. As we see next, ambiguity-aware beamforming can also improve target identifiability, i.e., for the same number of antennas, we can track more targets.

Example 6 (Target Identifiability). Consider again the scenario of Example 5 with N uniformly spaced antennas and K uniformly spaced targets. However, this time we allow K and N to differ. We are interested in the maximum number of identifiable targets, which we denote by $K^{\star}$ and define formally
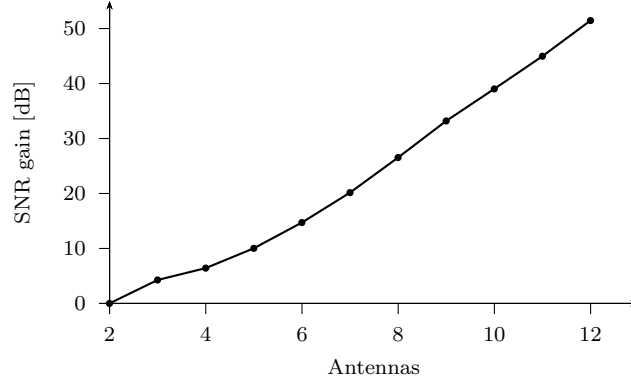
Fig. 4. Improvement in transmit power gain of beamforming for partial ambiguity over complete ambiguity as a function of number of antennas N.
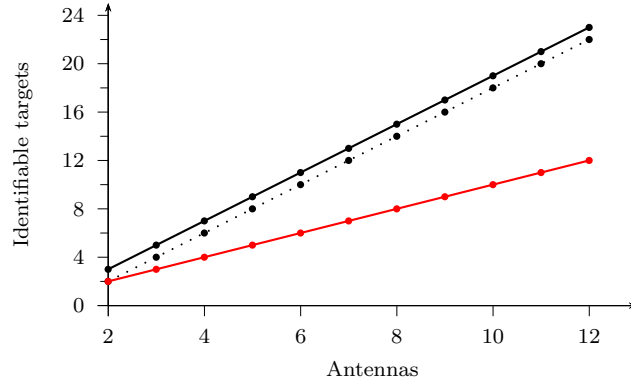

Fig. 5. Number of identifiable targets $K^\star$ as a function of number of antennas N for complete ambiguity (–) and partial ambiguity (exact numerical value – and analytical lower bound $\cdot\cdot$).

as the largest K for which the optimization problem (7) has a solution.

We compare again the complete ambiguity graph and the partially connected ambiguity graph with edges only between neighboring targets as introduced in Example 3. For the complete graph we show analytically in Appendix B that $K^\star = N$ (see the solid red/gray curve in Fig. 5). In contrast, the solid black curve in Fig. 5 shows the numerically computed value of $K^\star$ for the partial graph. The figure suggests that the number of identifiable targets $K^\star$ is $2N - 1$, i.e., almost doubled. Thus, explicitly taking the target ambiguity into account can also yield a significant improvement in target identifiability that again increases with the problem size. $\diamond$

We next explore the structure of the solution to the ambiguity-aware beamforming problem. We start by introducing some additional notation.

Denote by $\boldsymbol{U}_k \in \mathbb{C}^{N \times (N - |\mathcal{E}_k|)}$ a matrix whose columns are an orthonormal basis for the orthogonal complement of the subspace spanned by $\{\boldsymbol{a}(\theta_{k'})\}_{k' \in \mathcal{E}_k}$. In other words, $\boldsymbol{U}_k^\dagger \boldsymbol{U}_k = \boldsymbol{I}$, and $\boldsymbol{U}_k^\dagger \boldsymbol{a}(\theta_{k'}) = \boldsymbol{0}$ for all $k' \in \mathcal{E}_k$. Further, denote by $\boldsymbol{V}_k \in \mathbb{C}^{N \times (N-1)}$ a matrix whose columns are an orthonormal basis for the orthogonal complement of the subspace spanned by $\boldsymbol{a}(\theta_k)$. In other words, $\boldsymbol{V}_k^\dagger \boldsymbol{V}_k = \boldsymbol{I}$, and $\boldsymbol{V}_k^\dagger \boldsymbol{a}(\theta_k) = \boldsymbol{0}$. The choice of $\boldsymbol{U}_k$ and $\boldsymbol{V}_k$ is not unique; any such matrices will work for our purposes.

Consider then the matrix

$$\boldsymbol{R}(\boldsymbol{F}_k, \boldsymbol{G}_k) \triangleq \boldsymbol{U}_k \boldsymbol{F}_k \boldsymbol{U}_k^\dagger + \boldsymbol{V}_k \boldsymbol{G}_k \boldsymbol{V}_k^\dagger, \tag{9}$$

where $\boldsymbol{F}_k \in \mathbb{C}^{(N - |\mathcal{E}_k|) \times (N - |\mathcal{E}_k|)}$ and $\boldsymbol{G}_k \in \mathbb{C}^{(N-1) \times (N-1)}$ are arbitrary positive semidefinite matrices. Note that $\boldsymbol{R}(\boldsymbol{F}_k, \boldsymbol{G}_k)$ is positive semidefinite. For any k and $k' \in \mathcal{E}_k$,

$$\boldsymbol{a}^\dagger(\theta_k) \boldsymbol{R}(\boldsymbol{F}_k, \boldsymbol{G}_k) \boldsymbol{a}(\theta_{k'}) = \boldsymbol{a}^\dagger(\theta_k) \boldsymbol{U}_k \boldsymbol{F}_k \boldsymbol{U}_k^\dagger \boldsymbol{a}(\theta_{k'}) + \boldsymbol{a}^\dagger(\theta_k) \boldsymbol{V}_k \boldsymbol{G}_k \boldsymbol{V}_k^\dagger \boldsymbol{a}(\theta_{k'})$$

$$= \boldsymbol{a}^\dagger(\theta_k)\boldsymbol{U}_k\boldsymbol{F}_k\boldsymbol{0} + \boldsymbol{0}^\dagger\boldsymbol{G}_k\boldsymbol{V}_k^\dagger\boldsymbol{a}(\theta_{k'})$$
$$= 0,$$

and for any k

$$\boldsymbol{a}^\dagger(\theta_k)\boldsymbol{R}(\boldsymbol{F}_k, \boldsymbol{G}_k)\boldsymbol{a}(\theta_k) = \boldsymbol{a}^\dagger(\theta_k)\boldsymbol{U}_k\boldsymbol{F}_k\boldsymbol{U}_k^\dagger\boldsymbol{a}(\theta_k).$$

Further,

$$\begin{aligned}
\mathrm{tr}\big(\boldsymbol{R}(\boldsymbol{F}_k, \boldsymbol{G}_k)\big) &= \mathrm{tr}\big(\boldsymbol{U}_k\boldsymbol{F}_k\boldsymbol{U}_k^\dagger\big) + \mathrm{tr}\big(\boldsymbol{V}_k\boldsymbol{G}_k\boldsymbol{V}_k^\dagger\big) \\
&= \mathrm{tr}\big(\boldsymbol{U}_k^\dagger\boldsymbol{U}_k\boldsymbol{F}_k\big) + \mathrm{tr}\big(\boldsymbol{V}_k^\dagger\boldsymbol{V}_k\boldsymbol{G}_k\big) \\
&= \mathrm{tr}(\boldsymbol{F}_k) + \mathrm{tr}(\boldsymbol{G}_k).
\end{aligned}$$

From this discussion, we see that one way to construct a beamforming matrix $\boldsymbol{R}$ is to choose $\boldsymbol{F}_k$, $\boldsymbol{G}_k$ for $k \in \{1, 2, \ldots, K\}$ such that

$$\boldsymbol{R} = \boldsymbol{R}(\boldsymbol{F}_1, \boldsymbol{G}_1) = \cdots = \boldsymbol{R}(\boldsymbol{F}_K, \boldsymbol{G}_K),$$

and so that the constraint $\mathrm{tr}(\boldsymbol{R}) = 1$ is satisfied. Formally, a (potentially suboptimal) solution to the ambiguity-aware beamforming problem (7) can be found by solving:

$$\begin{aligned}
\underset{\boldsymbol{F}_k, \boldsymbol{G}_k \, \forall k}{\text{maximize}} \quad & \underset{k \in \{1,2,\ldots,K\}}{\min} \boldsymbol{a}^\dagger(\theta_k)\boldsymbol{U}_k\boldsymbol{F}_k\boldsymbol{U}_k^\dagger\boldsymbol{a}(\theta_k) \\
\text{subject to} \quad & \boldsymbol{R}(\boldsymbol{F}_k, \boldsymbol{G}_k) = \boldsymbol{R}(\boldsymbol{F}_1, \boldsymbol{G}_1), \quad \text{for all } k, \\
& \mathrm{tr}(\boldsymbol{F}_1) + \mathrm{tr}(\boldsymbol{G}_1) = 1, \\
& \boldsymbol{F}_k \succeq 0, \qquad\qquad \text{for all } k, \\
& \boldsymbol{G}_k \succeq 0, \qquad\qquad \text{for all } k.
\end{aligned} \tag{10}$$

This reformulation allows to obtain analytical insight into the structure of the solution to the ambiguity-aware beamforming problem as the next two examples illustrate.

Example 7 (Comparison with [8]). Let $N = K$ and consider a scenario with a complete ambiguity graph. Then the matrix $\boldsymbol{U}_k \in \mathbb{C}^{N \times (N - |\mathcal{E}_k|)} = \mathbb{C}^{N \times 1}$ is in fact simply a vector $\boldsymbol{u}_k$, and the matrix $\boldsymbol{F}_k$ is simply a positive scalar f_k. Thus,

$$\boldsymbol{R}(f_k, \boldsymbol{G}_k) = f_k\boldsymbol{u}_k\boldsymbol{u}_k^\dagger + \boldsymbol{V}_k\boldsymbol{G}_k\boldsymbol{V}_k^\dagger.$$

We need to ensure that

$$\boldsymbol{R}(f_1, \boldsymbol{G}_1) = \cdots = \boldsymbol{R}(f_K, \boldsymbol{G}_K).$$

Fix a target k and consider another target $k' \neq k$. Since the ambiguity graph is complete, $\boldsymbol{u}_{k'}$ is orthogonal to $\boldsymbol{a}_k$. Since the columns of $\boldsymbol{V}_k$ span the orthogonal complement of the subspace spanned by $\boldsymbol{a}_k$, this implies that $\boldsymbol{u}_{k'}$ can be written as $\boldsymbol{V}_k\boldsymbol{\nu}_{k,k'}$ for some $\boldsymbol{\nu}_{k,k'}$. Set

$$\boldsymbol{G}_k \triangleq \sum_{k' \neq k} f_{k'}\boldsymbol{\nu}_{k,k'}\boldsymbol{\nu}_{k,k'}^\dagger.$$

Then

$$\begin{aligned}
\boldsymbol{R}(f_k, \boldsymbol{G}_k) &= f_k\boldsymbol{u}_k\boldsymbol{u}_k^\dagger + \sum_{k' \neq k} f_{k'}\boldsymbol{V}_k\boldsymbol{\nu}_{k,k'}\boldsymbol{\nu}_{k,k'}^\dagger\boldsymbol{V}_k^\dagger \\
&= \sum_{k'=1}^{K} f_{k'}\boldsymbol{u}_{k'}\boldsymbol{u}_{k'}^\dagger,
\end{aligned}$$

which is identical for all k as required. The values of $f_{k'}$ can now be chosen to satisfy the trace constraint and to maximize the transmit power gain. This corresponds to the beamforming solution proposed in [8].[2] Thus, for the special case of complete ambiguity graphs, the solution to (10) reduces to the one in [8]. $\Diamond$

Example 6 (Identifiability Gain, Continued). We continue Example 6, and assume for the moment that K is even. As we had seen in Example 7, for the case of complete ambiguity graphs, the beamforming problem and its solution reduce to the one in [8]. Further, as argued in Appendix B, the largest number of identifiable targets $K^\star$ is equal to N in this case.

Consider then the case of a partial ambiguity graph with edges only between neighboring targets as defined in Example 3. Construct the positive semidefinite matrix

$$\boldsymbol{R} \triangleq \frac{1}{2N-K}\tilde{\boldsymbol{U}}_1\tilde{\boldsymbol{U}}_1^\dagger + \frac{1}{2N-K}\tilde{\boldsymbol{U}}_2\tilde{\boldsymbol{U}}_2^\dagger,$$

where the columns of $\tilde{\boldsymbol{U}}_1 \in \mathbb{C}^{N\times(N-K/2)}$ are an orthonormal basis for the orthogonal complement of the space spanned by $\boldsymbol{a}(\theta_k)$ with k odd, and where the columns of $\tilde{\boldsymbol{U}}_2 \in \mathbb{C}^{N\times(N-K/2)}$ are an orthonormal basis for the orthogonal complement of the space spanned by $\boldsymbol{a}(\theta_k)$ with k even. Observe that this is of a form similar to (9). This construction ensures that $\boldsymbol{a}^\dagger(\theta_k)\boldsymbol{R}\boldsymbol{a}(\theta_{k+1}) = 0$, satisfying the zero-forcing constraint between neighboring targets. Further, it is easily seen that $\mathrm{tr}(\boldsymbol{R}) = 1$ as required.

In general, this construction is possible as long as $N - K/2 \geq 1$. In other words, we can identify up to $2N-2$ targets, i.e., $K^\star \geq 2N-2$. This is shown as the dashed black curve in Fig. 5. It should be compared to the value of $K^\star$ of $2N-1$ obtained numerically shown as the solid black curve in Fig. 5. $\Diamond$

IV. AMBIGUITY-AWARE ASSOCIATION AND PARETO-OPTIMAL AMBIGUITY GRAPHS

So far, we have assumed that the ambiguity graph G is given (defined through (4) by the gates $\mathcal{S}_k \subset \mathbb{R}^2$). In Section III, we have seen how to solve the ambiguity-aware beamforming problem (7), which maximizes the transmit power gain $\boldsymbol{a}^\dagger(\theta_k)\boldsymbol{R}\boldsymbol{a}(\theta_k)$ for the worst-case target k as a function of the ambiguity graph G. Denote by $P(G)$ the value of this objective function for the optimal beamforming design.

We now turn to the problem of designing the ambiguity graph itself, or, equivalently, the gating sets $\{\mathcal{S}_k\}_{k=1}^K$, for the given prior distributions on the target parameters. Recall that our association rule is to find all detections with received filter tuned to azimuth angle θ_k falling into the gate $\mathcal{S}_k$. If there is a single such detection, the rule assigns it to track k. Otherwise, the rule declares an association error. Correct association occurs if the association rule runs to completion (i.e., does not declare an association error) and assigns each detection to the correct target.

Assume for the moment that the received signal is noiseless and a detection threshold of zero is used. The probability of detection error is then equal to zero. Further, making use of the zero-forcing constraint (6), we can lower bound the probability of correct association by the quantity

$$\begin{aligned}
C(G) &\triangleq \mathbb{P}\big((\tau_k,\omega_k) \in \mathcal{S}_k, (\tau_{k'},\omega_{k'}) \notin \mathcal{S}_k \ \forall k \text{ and } \forall k' \notin \mathcal{E}_k\big) \\
&= \mathbb{P}\big((\tau_k,\omega_k) \in \mathcal{S}_k \text{ for all } k\big),
\end{aligned} \tag{11}$$

where the second equality follows from the definition of $\mathcal{E}_k$ in (4). The randomness in this expression is due to τ_k and ω_k being random variables with distributions given by the prior.

Now consider noisy received signals. In this case, the probability of error can be upper bounded by the sum of two terms: The first term is an upper bound on the probability of detection error and is a decreasing function of the power gain $P(G)$ as mentioned in Section III. The second term is $1 - C(G)$, capturing the performance of the association rule.

There is a trade-off between these two terms: Choosing G to increase $P(G)$ causes to decrease $C(G)$. At one extreme consider the complete graph G containing all $K(K-1)/2$ edges. For this graph, the received filter tuned to a particular azimuth angle θ_k nulls out the interference of all other targets $k' \neq k$.

---

[2]To be precise, [8] sets $f_k \triangleq f$ for all k with f chosen to satisfy the trace constraint.
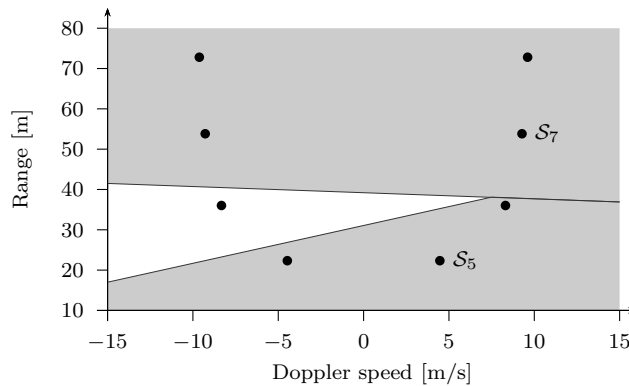
Fig. 6. Illustration of ambiguity-aware nearest-neighbor gating sets $\mathcal{S}_k$ for the graph in Fig. 2. For clarity, only two gating sets $\mathcal{S}_5$ and $\mathcal{S}_7$ are shown. Since the targets 5 and 7 are not connected by an edge in the graph in Fig. 2, the corresponding gating sets are disjoint. The figure assumes equal-variance Gaussian priors, resulting in convex polygonal regions. However, the definition of $\mathcal{S}_k$ applies to arbitrary prior distributions, and the resulting regions are neither polygons nor convex in general. This figure can be compared to the standard nearest-neighbor gates shown in Fig. 1.

Therefore, the association problem becomes simple, and the probability of correct association $C(G)$ is large. However, since we need to create beams with $K(K-1)/2$ nulls, the optimization problem (7) is maximally constrained and hence the optimal transmit power gain $P(G)$ is minimized. At the other extreme, consider the empty graph G containing no edges. For this graph, the beams can be chosen without any nulling constraints. Therefore, the transmit power gain $P(G)$ is maximized. However, the received filter tuned to a particular azimuth angle θ_k contains interference from all other targets $k' \neq k$. Therefore, the association problem is difficult, and the probability of correct association $C(G)$ is small.

Formally, the detection-association trade-off is given by the set of all Pareto-optimal[3] pairs of the form $\big(P(G), C(G)\big)$ parameterized by graphs G with vertices $\{1, 2, \ldots, K\}$. We call an ambiguity graph G optimal, if the corresponding pair $\big(P(G), C(G)\big)$ is Pareto optimal. Since there are $2^{K(K-1)/2}$ possible graphs with vertices $\{1, 2, \ldots, K\}$, finding optimal ambiguity graphs represents a computationally non-trivial combinatorial optimization problem. We next describe a design heuristic for constructing close to optimal ambiguity graphs.

For the expression (11) to be well defined, we need to describe how to choose the gating sets $\{\mathcal{S}_k\}_{k=1}^{K}$ corresponding to the ambiguity graph G. In order for the two to be consistent, we need $\mathcal{S}_k \cap \mathcal{S}_{k'} = \emptyset$ for all k and $k' \notin \mathcal{E}_k$ (see (4)). We introduce here an extension of the nearest-neighbor gating sets seen in Example 2. Define

$$\mathcal{S}_{k,k'} \triangleq \big\{ (\tau, \omega) : f_k(\tau, \omega) > f_{k'}(\tau, \omega) \big\}, \tag{12}$$

where $f_k(\tau, \omega)$ is the probability density for the prior on (τ_k, ω_k). Further, define

$$\mathcal{S}_k \triangleq \bigcap_{k' \notin \mathcal{E}_k} \mathcal{S}_{k,k'} = \Big\{ (\tau, \omega) : f_k(\tau, \omega) > \max_{k' \notin \mathcal{E}_k} f_{k'}(\tau, \omega) \Big\}$$

as the set of (τ, ω) pairs that are more likely to occur from target k than from any of the non-neighboring targets k' in the graph G. See Fig. 6 for an illustration. Clearly, $\mathcal{S}_k \cap \mathcal{S}_{k'} = \emptyset$ for all k and $k' \notin \mathcal{E}_k$, as required.

With this choice of gates $\mathcal{S}_k$, our generic association rule recalled at the beginning of this section can be rewritten (after some algebra) more compactly as in Algorithm 1. Since the maximizing k' in the inner-most loop can be computed in $O(K)$ time, the entire algorithm has run time $O(K^3)$. We refer to this association rule as *ambiguity-aware nearest-neighbor association*. We use this association rule for the evaluation of $C(G)$.

---

[3] A pair $\big(P(G), C(G)\big)$ is Pareto optimal if no other pair dominates it, meaning that there exists no other graph G' such that simultaneously $P(G') \geq P(G)$ and $C(G') \geq C(G)$, with at least one of the two inequalities being strict.

Algorithm 1 Ambiguity-aware nearest-neighbor association

> **for all** filter tracks k **do**
>> **for all** detections $(\hat{\tau}, \hat{\omega})$ with matched filter output $|r(\hat{\tau}, \hat{\omega}, \theta_k)|$ larger than threshold **do**
>>> **if** $\arg\max_{k' \notin \mathcal{E}_k} f_{k'}(\hat{\tau}, \hat{\omega}) = k$ **then**
>>>> assign detection $(\hat{\tau}, \hat{\omega})$ to filter track k
>>> **end if**
>> **end for**
> **end for**

(a) $N = 4$ antennas and $K = 4$ targets.
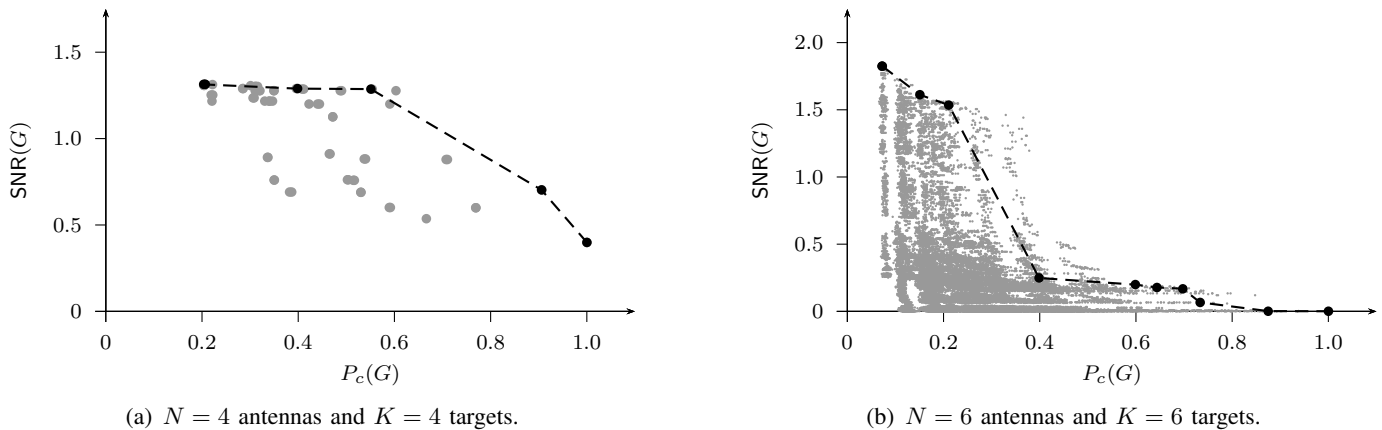
(b) $N = 6$ antennas and $K = 6$ targets.

Fig. 7. Detection-association trade-off for two settings with targets positioned as in Fig. 2. All values of $C(G)$ are numerically evaluated through Monte-Carlo integration. The black dots indicate the $\big(P(G_\gamma), C(G_\gamma)\big)$ pairs for different values of the threshold parameter γ. The gray dots are an exhaustive enumeration of $\big(P(G), C(G)\big)$ for all $2^{K(K-1)/2}$ (equal to 64 for $K = 4$ and equal to $32\,768$ for $K = 6$) possible ambiguity graphs G. Note that the trade-off curve can be convexified by time sharing (not shown in the figure).

Continuing from (11), we can now lower bound $C(G)$ using the union bound as

$$
\begin{aligned}
C(G) &\geq \mathbb{P}\big((\tau_k, \omega_k) \in \cap_{k' \notin \mathcal{E}_k} \mathcal{S}_{k,k'} \text{ for all } k\big) \\
&= 1 - \mathbb{P}\big((\tau_k, \omega_k) \in \cup_{k' \notin \mathcal{E}_k} \mathcal{S}_{k,k'}^{\mathsf{C}} \text{ for some } k\big) \\
&\geq 1 - K^2 \max_{(k,k'):k' \notin \mathcal{E}_k} \mathbb{P}\big((\tau_k, \omega_k) \notin \mathcal{S}_{k,k'}\big).
\end{aligned}
\tag{13}
$$

This last lower bound is a function of only the most difficult to disambiguate pair of targets (k, k') not connected by an edge in the ambiguity graph G.

Our design heuristic for choosing the graph G is as follows. Instead of optimizing $\big(P(G), C(G)\big)$ directly, we use the lower bound (13) on $C(G)$ as a substitute. With this substitution, the optimizing G can be readily found. Observe that $P(G)$ does not decrease (and usually increases) whenever we remove an edge from G. At the same time, (13) stays constant whenever we remove an edge from G that is not achieving the maximum probability of pairwise error. This implies that all optimal (for the modified criterion) ambiguity graphs have edge sets of the form

$$
\mathcal{E}_k = \big\{ k' \neq k : \mathbb{P}\big((\tau_k, \omega_k) \in \mathcal{S}_{k,k'}\big) \leq \gamma \big\}
\tag{14}
$$

for some threshold parameter γ and with $\mathcal{S}_{k,k'}$ as defined in (12). In words, all target pairs that are pairwise more difficult to disambiguate than the threshold parameter γ form an edge in the ambiguity graph. Let G_γ be the corresponding graph. By sweeping γ from 0 to 1, we create a sequence of up to $K(K-1)/2$ optimal graphs G_γ, which in turn trace out the detection-association trade-off $\big(P(G_\gamma), C(G_\gamma)\big)$. Fig. 7 shows two examples of this approach. The figure indicates that the proposed design heuristic can be quite close to optimal.

To summarize this section, our proposed approach is as follows. Fix a value of the threshold parameter γ to some value between 0 and 1 depending on the application requirements. Construct the corresponding ambiguity graph G_γ with edges given by (14). Solve the corresponding optimal ambiguity-aware beamforming problem (7) and steer the radar beams accordingly. From the radar returns, find all the detections and associate them using the nearest-neighbor association rule in Algorithm 1 parameterized by the graph G_γ.

V. DISCUSSION AND CONCLUSION

In this paper, we studied the problem of jointly designing transmit beam patterns and association rules for tracking multiple targets using MIMO radar. We introduced the concept of the ambiguity graph used to describe which targets are hard to disambiguate based on prior information. We first formulated a semidefinite program to solve the problem of designing beam patterns that avoid simultaneous illumination of hard to disambiguate targets. We then designed the association rule assigning detections to the different targets being tracked. Finally, we solved the problem of designing ambiguity graphs by using a heuristic to approximate the optimal detection-association trade-off.

In our analysis we made a number of simplifying assumptions. Some of these can be readily relaxed. For instance, the ambiguity-aware beamforming problem (7) completely nulls interfering target signal contributions, i.e., $\boldsymbol{a}^\dagger(\theta_k)\boldsymbol{Ra}(\theta_{k'}) = 0$ for all k and all $k' \in \mathcal{E}_k$. This constraint may be too restrictive, and it may be sufficient to ensure that the interfering target signals are below the noise floor, i.e., $|\boldsymbol{a}^\dagger(\theta_k)\boldsymbol{Ra}(\theta_{k'})| \leq \delta$ for all k and all $k' \in \mathcal{E}_k$ with $\delta > 0$. The resulting optimization problem remains convex and can be solved efficiently.

Similarly, we have assumed that the target azimuth angles are known a priori. To relax this, assume that we have prior upper and lower bounds θ_k^- and θ_k^+ on each target azimuth θ_k. The ambiguity-aware beamforming problem (7) can be modified to accommodate this uncertainty by replacing the objective with $\min_{k \in \{1,2,\ldots,K\}} \min_{\theta \in [\theta_k^-, \theta_k^+]} \boldsymbol{a}^\dagger(\theta)\boldsymbol{Ra}(\theta)$ and the constraints with $\max_{\theta \in [\theta_k^-, \theta_k^+]} \max_{\theta' \in [\theta_{k'}^-, \theta_{k'}^+]} |\boldsymbol{a}^\dagger(\theta)\boldsymbol{Ra}(\theta')| \leq \delta$ for all k and all $k' \in \mathcal{E}_k$. Here $\delta > 0$ is a small but strictly positive number that controls the amount of interference as discussed in the last paragraph. This optimization problem is again convex.

There are several directions for future work. Our analysis assumed that the ambiguity function is ideal, and we have argued how to construct corresponding waveforms in the large-bandwidth regime. Joint beamforming and association design under nonideal ambiguity function is an interesting open problem. Further, while we have jointly solved the beamforming and association problems, we have not directly considered the tracking problem. Solving all three problems jointly is an interesting direction for future work involving several new aspects such as how to handle association failures and how to initiate tracks.

APPENDIX A
WAVEFORMS WITH APPROXIMATELY IDEAL AMBIGUITY FUNCTION

We construct waveforms of support $[0, T)$ and (approximate) bandwidth B that have close to ideal ambiguity function $\boldsymbol{\chi}(\Delta\tau, \Delta\omega)$ as defined in (2). We formally state the result as the following theorem.

Theorem 1. *Let* $\delta > 0$ *with* $1/\delta \in \mathbb{N}$, *and let* $T > 0$, $B > 0$ *with* $BT \in \mathbb{N}$, *satisfying*

$$2^{-8}\delta^2 BT - 2\ln(BT) > \ln(2^9 N^2/\delta^3). \tag{15}$$

There exists waveforms $\tilde{\boldsymbol{s}}(t) \in \mathbb{C}^N$ *of support* $[0, T)$ *and approximate (i.e., Rayleigh or equivalently half the null-to-null) bandwidth* B *with ambiguity function* $\boldsymbol{\chi}(\Delta\tau, \Delta\omega) \in \mathbb{C}^{N \times N}$ *having the following properties:*

1) $\chi_{n,n}(0,0) = 1$
   for all $n \in \{1, 2, \ldots, N\}$.

2) $|\chi_{n,n}(\Delta\tau, \Delta\omega)| \leq \delta$
   for all $n \in \{1, 2, \ldots, N\}$ *and for all* $\Delta\tau, \Delta\omega \in \mathbb{R}$ *with either* $|\Delta\tau| \geq 1/B$ *or* $26/(\delta T) \leq |\Delta\omega| \leq \pi B$.
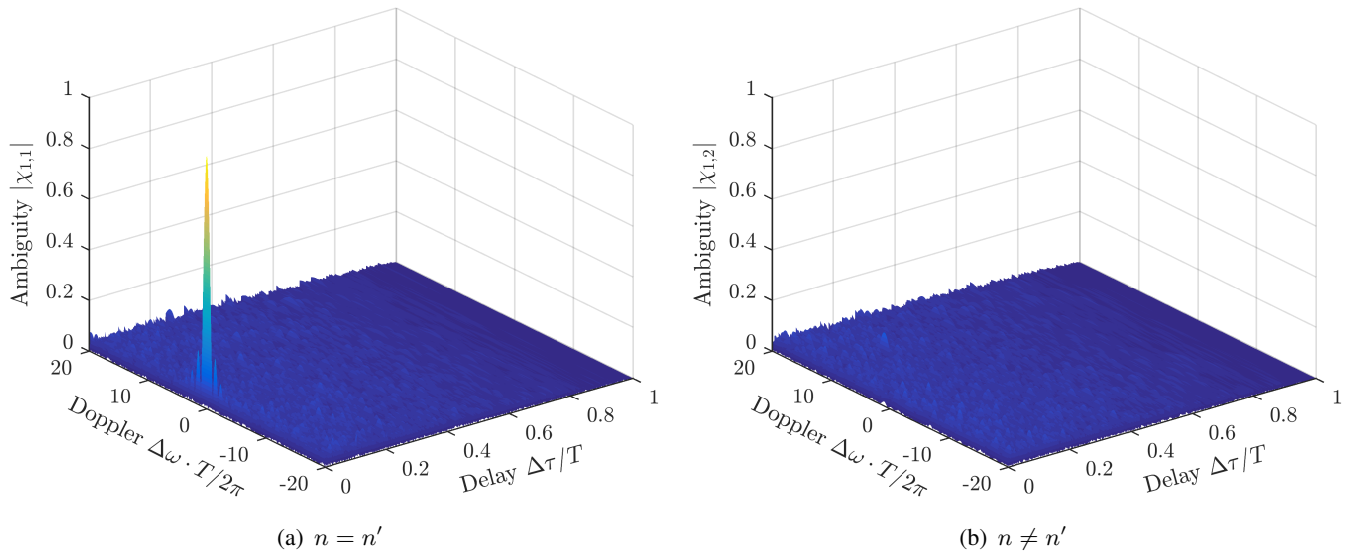
Fig. 8. Ambiguity function for randomly constructed waveforms $\tilde{s}(t)$ as in Theorem 1 with temporal support $T = 1\,\mathrm{s}$ and bandwidth $B = 10^3\,\mathrm{Hz}$. Notice that even for this relatively low bandwidth, the ambiguity function is already quite close to ideal.

3) $|\chi_{n,n'}(\Delta\tau, \Delta\omega)| \leq \delta$
   for all $n, n' \in \{1, 2, \ldots, N\}$ with $n \neq n'$ and for all $\Delta\tau, \Delta\omega \in \mathbb{R}$.

While Theorem 1 only proves existence of such a set of waveforms, the proof shows that if BT is slightly larger than the minimum necessary to satisfy (15), then the vast majority of waveforms generated by the randomized construction described below will have the above properties. The ambiguity function for one such set of waveforms generated at random is shown in Fig. 8.

Example 8. For a numerical example, consider temporal support $T = 1\,\mathrm{s}$, bandwidth $B = 1\,\mathrm{GHz}$, and $N = 16$ antennas. Then the condition (15) is satisfied for any side-lobe level of $\delta \geq -23\,\mathrm{dB}$. Choosing $\delta = -10\,\mathrm{dB}$, and assuming a carrier frequency of $77\,\mathrm{GHz}$, the limits on $\Delta\tau$ and $\Delta\omega$ imposed by Property 2 in Theorem 1 translate into a range resolution of $0.15\,\mathrm{m}$ and a Doppler velocity resolution of $0.16\,\mathrm{m/s}$ with an upper bound of $1.9 \times 10^6\,\mathrm{m/s}$. $\diamond$

Proof of Theorem 1: As alluded to above, we use a randomized construction. Let $c_{n,\ell}$ with $n \in \{1, 2, \ldots, N\}$ and $\ell \in \{0, 1, \ldots, BT-1\}$ be independent random variables uniformly distributed over the complex unit circle. Set

$$\tilde{s}_n(t) \triangleq \frac{1}{\sqrt{T}} \sum_{\ell=0}^{BT-1} c_{n,\ell} 1_{[0,1/B)}(t - \ell/B), \tag{16}$$

where $1_{\mathcal{D}}(t)$ denotes the indicator function for the set $\mathcal{D} \subset \mathbb{R}$, i.e.,

$$1_{\mathcal{D}}(t) \triangleq \begin{cases} 1, & \text{if } t \in \mathcal{D}, \\ 0, & \text{if } t \notin \mathcal{D}. \end{cases}$$

In words, $\tilde{s}_n(t)$ is piece-wise constant over intervals of length $1/B$, and the value on each such interval is uniformly distributed over the complex circle with magnitude $1/\sqrt{T}$. These waveforms therefore fall into the class of polyphase codes [3, Section 4.10.2]. Clearly, $\tilde{s}_n(t)$ has support $t \in [0, T)$. Further, since each term $1_{[0,1/B)}(t - \ell/B)$ in $\tilde{s}_n(t)$ has approximate bandwidth B, so does $\tilde{s}_n(t)$ itself.

We next analyze the entries $\chi_{n,n'}(\Delta\tau, \Delta\omega)$ of the ambiguity function. By symmetry of the ambiguity function, we can assume without loss of generality that $\Delta\tau \geq 0$. The analysis proceeds in three main steps. In the first step, we argue that all waveforms of the above type have the desired ambiguity properties for

$n' = n$ and $\Delta\tau = \Delta\omega = 0$ and for all large enough $|\Delta\tau|$ and $|\Delta\omega|$. In the second step, we argue that a set of waveforms randomly generated as above has the desired ambiguity properties with positive probability at all sample points $(\Delta\tau, \Delta\omega)$ of the form $\Delta\tau = J\delta/(8B)$ and $\Delta\omega = M\delta/T$ for integer J, M. Hence, there exists at least one such set of waveforms. In the third step, we argue that if a set of waveforms has the desired ambiguity properties at all the sample points, then it also has them at all points in between.

Before proceeding to the main arguments we present the following two technical lemmas that we will use throughout the proof.

Lemma 2. *Let* $n, n' \in \{1, 2, \ldots, N\}$, $\varepsilon \in [0, 1]$, $L \in \{0, 1, 2, \ldots\}$, *and* $\Delta\omega \in \mathbb{R}$. *Then* $\chi_{n,n'}$ *can be expanded as*

$$\chi_{n,n'}\big((L+\varepsilon)/B, \Delta\omega\big) = \frac{1}{T} \sum_{\ell=L}^{BT-1} c_{n,\ell}\big(c_{n',\ell-L}^* a(\ell, \varepsilon, \Delta\omega) + c_{n',\ell-(L+1)}^* b(\ell, \varepsilon, \Delta\omega)\big), \tag{17}$$

where

$$a(\ell, \varepsilon, \Delta\omega) \triangleq \int_{t=(\ell+\varepsilon)/B}^{(\ell+1)/B} \exp(-j\Delta\omega t)\, dt,$$

$$b(\ell, \varepsilon, \Delta\omega) \triangleq \int_{t=\ell/B}^{(\ell+\varepsilon)/B} \exp(-j\Delta\omega t)\, dt,$$

and with the convention that $c_{n',-1} \triangleq 0$. *Furthermore,*

$$|a(\ell, \varepsilon, \Delta\omega)| \leq \min\{2/|\Delta\omega|, 1/B\},$$
$$|b(\ell, \varepsilon, \Delta\omega)| \leq \min\{2/|\Delta\omega|, 1/B\}.$$

Proof: We have

$$\chi_{n,n'}\big((L+\varepsilon)/B, \Delta\omega\big)$$
$$= \int_{t=(L+\varepsilon)/B}^{T} \tilde{s}_n(t)\tilde{s}_{n'}^*\big(t - (L+\varepsilon)/B\big) \exp(-j\Delta\omega t)\, dt$$
$$= \frac{1}{T} \sum_{\ell=L}^{BT-1} c_{n,\ell}\bigg(c_{n',\ell-L}^* \int_{t=(\ell+\varepsilon)/B}^{(\ell+1)/B} \exp(-j\Delta\omega t)\, dt + c_{n',\ell-(L+1)}^* \int_{t=\ell/B}^{(\ell+\varepsilon)/B} \exp(-j\Delta\omega t)\, dt\bigg)$$
$$= \frac{1}{T} \sum_{\ell=L}^{BT-1} c_{n,\ell}\big(c_{n',\ell-L}^* a(\ell, \varepsilon, \Delta\omega) + c_{n',\ell-(L+1)}^* b(\ell, \varepsilon, \Delta\omega)\big),$$

proving the first part of the lemma. The second part follows from

$$\left|\int_{t=x}^{y} \exp(-j\Delta\omega t)\, dt\right| = \frac{1}{|\Delta\omega|}\big|\exp(-j\Delta\omega y) - \exp(-j\Delta\omega x)\big|$$
$$\leq \frac{2}{|\Delta\omega|}$$

and

$$\left|\int_{t=x}^{y} \exp(-j\Delta\omega t)\, dt\right| \leq \int_{t=x}^{y} \big|\exp(-j\Delta\omega t)\big|\, dt$$
$$= y - x,$$

both for $x \leq y$. ∎

Lemma 3. *Let* $n, n' \in \{1, 2, \ldots, N\}$, $\varepsilon \in [0, 1]$, $L \in \{0, 1, 2, \ldots\}$, *and* $\Delta\omega \in \mathbb{R}$ *as in Lemma 2. Then the terms in the expansion* (17) *of* $\chi_{n,n'}\big((L+\varepsilon)/B, \Delta\omega\big)$ *given in Lemma 2 satisfy the following for any* $\kappa > 0$.

1) *If either $n \neq n'$ or $L \geq 1$,*

$$\mathbb{P}\left(\left|\sum_{\ell=L}^{BT-1} c_{n,\ell}c^*_{n',\ell-L}a(\ell, \varepsilon, \Delta\omega)\right| > \kappa\right) \leq 4\exp\left(-\frac{\kappa^2 B}{4T}\right). \tag{18}$$

2) *For all n, n' and all $L \in \{0, 1, 2, \ldots\}$,*

$$\mathbb{P}\left(\left|\sum_{\ell=L}^{BT-1} c_{n,\ell}c^*_{n',\ell-(L+1)}b(\ell, \varepsilon, \Delta\omega)\right| > \kappa\right) \leq 4\exp\left(-\frac{\kappa^2 B}{4T}\right). \tag{19}$$

Proof: First assume that $L \geq 1$ or $n \neq n'$. To simplify notation, define

$$z_\ell \triangleq c_{n,\ell}c^*_{n',\ell-L}a(\ell, \varepsilon, \Delta\omega).$$

By the union bound,

$$\mathbb{P}\left(\left|\sum_{\ell=L}^{BT-1} z_\ell\right| > \kappa\right) \leq \mathbb{P}\left(\left|\sum_{\ell=L}^{BT-1} \Re\{z_\ell\}\right| > \kappa/\sqrt{2}\right) + \mathbb{P}\left(\left|\sum_{\ell=L}^{BT-1} \Im\{z_\ell\}\right| > \kappa/\sqrt{2}\right). \tag{20}$$

Since the random variables $c_{n,\ell}$ and $c_{n',\ell-L}$ are independent by assumption on L and n, n', the random variable z_ℓ has expected value zero. Moreover variables in the sequence z_ℓ indexed by $\ell \in \{L, L + 1, \ldots, BT - 1\}$ are mutually independent. (This last statement can be observed by considering the distribution of $c_{n,\ell}c^*_{n',\ell-L}$ conditioned on all $c_{n,\ell'}c^*_{n',\ell'-L}$ with $\ell' < \ell$, and by noticing that $c_{n,\ell}$ does not appear in the conditioning.) Furthermore, from the fact that $c_{n,\ell}$ is on the unit circle and the bound on the magnitude of $a(\ell, \varepsilon, \Delta\omega)$ from Lemma 2, we know that $|z_\ell| \leq 1/B$. We can therefore apply Hoeffding's inequality [25, Chapter 2.6] to both terms on the right-hand side of (20) to obtain

$$\mathbb{P}\left(\left|\sum_{\ell=L}^{BT-1} z_\ell\right| > \kappa\right) \leq 4\exp\left(-\frac{\kappa^2 B}{4T}\right).$$

This completes the proof of (18).

The proof of (19) follows similarly by noting that the random variable $c_{n,\ell}$ is independent of the random variables $c_{n',\ell-(L+1)}$ for all n' and all $L \geq 0$. ∎

We start with step one of the proof, which analyzes properties of all waveforms of the form (16). Consider first $n' = n$, $\Delta\tau = \Delta\omega = 0$. We then have

$$\chi_{n,n}(0, 0) = \int_{t=0}^{T} |\tilde{s}_n(t)|^2 \, dt = 1,$$

as required.

Consider next any n, n', $\Delta\tau \geq T$ and any $\Delta\omega \in \mathbb{R}$. Then clearly

$$\chi_{n,n'}(\Delta\tau, \Delta\omega) = 0, \tag{21}$$

since each waveform $\tilde{s}_n(t)$ has support $[0, T)$.

Consider next any n, n', $\Delta\tau \geq 0$, and $|\Delta\omega| \geq 4B/\delta$. Let $L \triangleq \lfloor \Delta\tau B \rfloor$ and $\varepsilon \triangleq \Delta\tau B - L$ so that $\Delta\tau = (L + \varepsilon)/B$. By Lemma 2,

$$\begin{aligned}
\left|\chi_{n,n'}(\Delta\tau, \Delta\omega)\right| &= \left|\chi_{n,n'}\big((L+\varepsilon)/B, \Delta\omega\big)\right| \\
&\leq \frac{1}{T}\sum_{\ell=L}^{BT-1}\big(|a(\ell, \varepsilon, \Delta\omega)| + |b(\ell, \varepsilon, \Delta\omega)|\big) \\
&\leq \frac{1}{T} \cdot BT \cdot \frac{4}{|\Delta\omega|} \\
&\leq \delta, \tag{22}
\end{aligned}$$

as needed. This concludes step one.

We proceed with step two of the proof, which analyzes properties valid with positive probability by waveforms of the form (16). Consider $\Delta\tau$ of the form $J\delta/(8B)$ with $J \in \{0, 1, 2, \ldots, \lfloor 8BT/\delta \rfloor\}$, and consider $\Delta\omega$ of the form $M\delta/T$ with $M \in \mathbb{Z}$. Let $L \triangleq \lfloor J\delta/8 \rfloor$ and $\varepsilon \triangleq J\delta/8 - L$ so that $J\delta/(8B) = (L + \varepsilon)/B$.

From Lemma 2, we have

$$
\begin{aligned}
\left| \chi_{n,n'}\big(J\delta/(8B), M\delta/T \big) \right| &= \left| \chi_{n,n'}\big((L + \varepsilon)/B, M\delta/T \big) \right| \\
&\leq \frac{1}{T} \left| \sum_{\ell=L}^{BT-1} c_{n,\ell} c_{n',\ell-L}^* a(\ell, \varepsilon, M\delta/T) \right| + \frac{1}{T} \left| \sum_{\ell=L}^{BT-1} c_{n,\ell} c_{n',\ell-(L+1)}^* b(\ell, \varepsilon, M\delta/T) \right| \\
&= \frac{1}{T} \left| \sum_{\ell=L}^{BT-1} x_\ell \right| + \frac{1}{T} \left| \sum_{\ell=L}^{BT-1} y_\ell \right|
\end{aligned}
\tag{23}
$$

with

$$
\begin{aligned}
x_\ell &\triangleq c_{n,\ell} c_{n',\ell-L}^* a(\ell, \varepsilon, M\delta/T), \\
y_\ell &\triangleq c_{n,\ell} c_{n',\ell-(L+1)}^* b(\ell, \varepsilon, M\delta/T).
\end{aligned}
$$

We now consider two cases separately, depending on the value of J and n, n'.

Case 1: $J \geq 8/\delta$ or $n \neq n'$. Observe that $J \geq 8/\delta$ implies $L \geq 1$. Hence, we can apply Lemma 3 with $\kappa \triangleq \delta T/8$ to both terms in the right-hand side of (23) to obtain

$$
\mathbb{P}\left(\frac{1}{T} \left| \sum_{\ell=J}^{BT-1} x_\ell \right| > \delta/8 \right) \leq 4 \exp\big(-2^{-8}\delta^2 BT\big)
$$

and

$$
\mathbb{P}\left(\frac{1}{T} \left| \sum_{\ell=J}^{BT-1} y_\ell \right| > \delta/8 \right) \leq 4 \exp\big(-2^{-8}\delta^2 BT\big).
$$

Hence

$$
\begin{aligned}
\mathbb{P}\left(\frac{1}{T} \left| \sum_{\ell=J}^{BT-1} x_\ell \right| + \frac{1}{T} \left| \sum_{\ell=J}^{BT-1} y_\ell \right| > \delta/4 \right) &\leq \mathbb{P}\left(\frac{1}{T} \left| \sum_{\ell=J}^{BT-1} x_\ell \right| > \delta/8 \right) + \mathbb{P}\left(\frac{1}{T} \left| \sum_{\ell=J}^{BT-1} y_\ell \right| > \delta/8 \right) \\
&\leq 8 \exp\big(-2^{-8}\delta^2 BT\big).
\end{aligned}
$$

Substituting into (23) yields that

$$
\mathbb{P}\Big(\left| \chi_{n,n'}\big(J\delta/(8B), M\delta/T \big) \right| \leq \delta/4 \Big) \geq 1 - 8 \exp\big(-2^{-8}\delta^2 BT\big).
\tag{24}
$$

Case 2: $J < 8/\delta$ and $n = n'$. In this case we have $L = 0$, so that $x_\ell = a(\ell, \varepsilon, M\delta/T)$. Moreover, since $n = n'$, we can restrict ourselves to $|\Delta\omega| \in \big[26/(\delta T), \pi B \big]$. We can upper bound the first term in the

right-hand side of (23) as

$$\frac{1}{T}\left|\sum_{\ell=L}^{BT-1} x_\ell\right| = \frac{1}{T}\left|\sum_{\ell=0}^{BT-1} a(\ell,\varepsilon,\Delta\omega)\right|$$

$$= \frac{1}{T}\left|\sum_{\ell=0}^{BT-1}\int_{t=(\ell+\varepsilon)/B}^{(\ell+1)/B}\exp(-j\Delta\omega t)\,dt\right|$$

$$= \frac{1}{T|\Delta\omega|}\left|\sum_{\ell=0}^{BT-1}\left(\exp\left(-j\Delta\omega\tfrac{\ell+1}{B}\right)-\exp\left(-j\Delta\omega\tfrac{\ell+\varepsilon}{B}\right)\right)\right|$$

$$= \frac{\left|\exp\left(-j\tfrac{\Delta\omega}{B}\right)-\exp\left(-j\tfrac{\Delta\omega\varepsilon}{B}\right)\right|}{T|\Delta\omega|}\left|\sum_{\ell=0}^{BT-1}\exp\left(-j\tfrac{\Delta\omega\ell}{B}\right)\right|$$

$$= \frac{\left|\left(\exp\left(-j\tfrac{\Delta\omega}{B}\right)-\exp\left(-j\tfrac{\Delta\omega\varepsilon}{B}\right)\right)\left(1-\exp(-j\Delta\omega T)\right)\right|}{T\left|\Delta\omega\left(1-\exp\left(-j\tfrac{\Delta\omega}{B}\right)\right)\right|}$$

$$= \frac{|(1-\exp(-j\Delta\omega T)|}{T|\Delta\omega|}\frac{\left|\sin\left(\tfrac{\Delta\omega(1-\varepsilon)}{2B}\right)\right|}{\left|\sin\left(\tfrac{\Delta\omega}{2B}\right)\right|}. \tag{25}$$

Since $|\Delta\omega| \leq \pi B$, we have $\Delta\omega/(2B) \in [-\pi/2, \pi/2]$. Using that $2|x|/\pi \leq |\sin(x)| \leq |x|$ for $x \in [-\pi/2, \pi/2]$, we can thus further upper bound (25) as

$$\frac{1}{T}\left|\sum_{\ell=L}^{BT-1} x_\ell\right| \leq \frac{2}{T|\Delta\omega|}\cdot\frac{1-\varepsilon}{2/\pi}$$

$$\leq \frac{\pi}{T|\Delta\omega|}$$

$$\overset{(a)}{\leq} \delta\pi/26$$

$$< \delta/8, \tag{26}$$

where (a) uses that $|\Delta\omega| \geq 26/(\delta T)$ by assumption.

For the second term in the right-hand side of (23) we make use of Lemma 3 with $\kappa \triangleq \delta T/8$ to obtain

$$\mathbb{P}\left(\frac{1}{T}\left|\sum_{\ell=J}^{BT-1} y_\ell\right| > \delta/8\right) \leq 4\exp\left(-2^{-8}\delta^2 BT\right). \tag{27}$$

We can combine (26) and (27) with (23) to yield

$$\mathbb{P}\left(\left|\chi_{n,n'}\left(J\delta/(8B), M\delta/T\right)\right| \leq \delta/4\right) \geq \mathbb{P}\left(\frac{1}{T}\left|\sum_{\ell=J}^{BT-1} x_\ell\right| + \frac{1}{T}\left|\sum_{\ell=J}^{BT-1} y_\ell\right| \leq \delta/4\right)$$

$$\geq 1 - 4\exp\left(-2^{-8}\delta^2 BT\right)$$

$$\geq 1 - 8\exp\left(-2^{-8}\delta^2 BT\right) \tag{28}$$

for $|M\delta/T| \in [26/(\delta T), \pi B]$.

Combining (24) from Case 1 and (28) from Case 2, we conclude that the inequality

$$\mathbb{P}\left(\left|\chi_{n,n'}(\Delta\tau, \Delta\omega)\right| \leq \delta/4\right) \geq 1 - 8\exp\left(-2^{-8}\delta^2 BT\right)$$

holds for all sample points $(\Delta\tau, \Delta\omega)$ of the form $\left(J\delta/(8B), M\delta/T\right)$ either when $n \neq n'$ or when $n = n'$ and $|\Delta\omega| = |M\delta/T| \in [26/(\delta T), \pi B]$.

Recall from (21) and (22) in step one that in this second step it suffices to consider values $\Delta\tau \in [0, T)$ and $\Delta\omega \in (-4B/\delta, 4B/\delta)$. There are at most $8BT/\delta$ possible values of $\Delta\tau$ of the form $J\delta/(8B)$ in $[0, T)$, at most $8BT/\delta^2$ possible values of $\Delta\omega$ of the form $M\delta/T$ in $(-4B/\delta, 4B/\delta)$, and N^2 possible values for $n, n' \in \{1, 2, \ldots, N\}$.[4] Hence, by the union bound, with probability at least

$$1 - \frac{8BT}{\delta} \cdot \frac{8BT}{\delta^2} \cdot N^2 \cdot 8\exp\left(-2^{-8}\delta^2 BT\right) = 1 - \frac{2^9 B^2 T^2 N^2}{\delta^3}\exp\left(-2^{-8}\delta^2 BT\right),$$

the ambiguity function at those sample points $(\Delta\tau, \Delta\omega)$ has magnitude at most $\delta/4$. If the condition

$$2^{-8}\delta^2 BT - 2\ln(BT) > \ln(2^9 N^2/\delta^3)$$

holds, then this probability is strictly positive. This implies that, under this condition, at least one set of waveforms having ambiguity function with magnitude less than $\delta/4$ at the sample points exists, concluding step two.

For step three of the proof, take the set of waveforms with small ($\leq \delta/4$) ambiguity at the sample points constructed in step two. Using a continuity argument, we will show that it has small ($\leq \delta$) ambiguity at all non-sample points as well.

We start with the continuity argument in the $\Delta\tau$-direction. Consider $J \in \mathbb{Z}$ and assume

$$\left|\chi_{n,n'}\left(J\delta/(8B), \Delta\omega\right)\right| \leq \delta/4.$$

Let $\eta \in [0, 1)$. We will argue that

$$\left|\chi_{n,n'}\left((J+\eta)\delta/(8B), \Delta\omega\right)\right| \leq \delta/2.$$

Set $L \triangleq \lfloor J\delta/8 \rfloor$ and $\varepsilon \triangleq J\delta/8 - L$, so that $J\delta/8 = L + \varepsilon$. Since $1/\delta \in \mathbb{N}$, all integer multiples of $1/B$ are also integer multiples of $\delta/(8B)$ and therefore sample points. Since η is strictly less than one, this implies that $\lfloor (J+\eta)\delta/8 \rfloor = L$. This observation allows us to apply Lemma 2 to write

$$\left|\chi_{n,n'}\left(\frac{(J+\eta)\delta}{8B}, \Delta\omega\right) - \chi_{n,n'}\left(\frac{J\delta}{8B}, \Delta\omega\right)\right|$$
$$= \left|\chi_{n,n'}\left(\frac{L+\varepsilon+\eta\delta/8}{B}, \Delta\omega\right) - \chi_{n,n'}\left(\frac{L+\varepsilon}{B}, \Delta\omega\right)\right|$$
$$= \frac{1}{T}\left|\sum_{\ell=L}^{BT-1} c_{n,\ell}\left(c_{n',\ell-L}^*\left(a(\ell, \varepsilon+\eta\delta/8, \Delta\omega) - a(\ell, \varepsilon, \Delta\omega)\right)\right.\right.$$
$$\left.\left. + c_{n',\ell-(L+1)}^*\left(b(\ell, \varepsilon+\eta\delta/8, \Delta\omega) - b(\ell, \varepsilon, \Delta\omega)\right)\right)\right|$$
$$\leq \frac{1}{T}\sum_{\ell=L}^{BT-1}\left|a(\ell, \varepsilon+\eta\delta/8, \Delta\omega) - a(\ell, \varepsilon, \Delta\omega)\right| + \frac{1}{T}\sum_{\ell=L}^{BT-1}\left|b(\ell, \varepsilon+\eta\delta/8, \Delta\omega) - b(\ell, \varepsilon, \Delta\omega)\right|$$
$$= \frac{BT}{T}\left|\int_{t=\varepsilon/B}^{(\varepsilon+\eta\delta/8)/B}\exp(-j\Delta\omega t)\,dt\right| + \frac{BT}{T}\left|\int_{t=\varepsilon/B}^{(\varepsilon+\eta\delta/8)/B}\exp(-j\Delta\omega t)\,dt\right|$$
$$\leq B\cdot\frac{2\eta\delta}{8B}$$
$$\leq \delta/4.$$

Hence, by the triangle inequality,

$$\left|\chi_{n,n'}\left((J+\eta)\delta/(8B), \Delta\omega\right)\right| \leq \left|\chi_{n,n'}\left(J\delta/(8B), \Delta\omega\right)\right| + \delta/4$$
$$\leq \delta/2. \tag{29}$$

---

[4]Recall that $1/\delta$ and BT are both in $\mathbb{N}$.

We continue with the continuity argument in the $\Delta\omega$-direction. Consider $M \in \mathbb{Z}$ and assume

$$|\chi_{n,n'}(\Delta\tau, M\delta/T)| \leq \delta/2.$$

Let $\eta \in [0, 1)$. Then

$$\left|\chi_{n,n'}\big(\Delta\tau, (M+\eta)\delta/T\big) - \chi_{n,n'}(\Delta\tau, M\delta/T)\right| \leq \frac{1}{T}\int_{t=0}^{T}|1 - \exp(-j\eta\delta t/T)|\,dt$$
$$\leq \frac{\delta}{T^2}\int_{t=0}^{T} t\,dt$$
$$= \delta/2.$$

Hence

$$\left|\chi_{n,n'}\big(\Delta\tau, (M+\eta)\delta/T\big)\right| \leq |\chi_{n,n'}(\Delta\tau, M\delta/T)| + \delta/2$$
$$\leq \delta. \tag{30}$$

Together, (29) and (30) show that all points $\Delta\omega$ between sample points have small ambiguity as well. This completes step three and the proof. ∎

APPENDIX B
NUMBER OF IDENTIFIABLE TARGETS FOR COMPLETE AMBIGUITY GRAPHS

In this appendix, we show that, for complete ambiguity graphs and for "general" $\boldsymbol{a}(\theta_k)$, the maximal number of identifiable targets is $K^\star = N$.

In Example 7, we have seen an explicit construction that allows to identify $K = N$ targets. Hence $K^\star \geq N$.

Conversely, assume that $K \geq N + 1$ and consider target k. Since the ambiguity graph is complete, we must have $\boldsymbol{a}^\dagger(\theta_k)\boldsymbol{R}\boldsymbol{a}(\theta_{k'}) = 0$ for all $k' \neq k$. This implies that $\boldsymbol{a}^\dagger(\theta_k)\boldsymbol{R}\boldsymbol{c} = 0$ for all $\boldsymbol{c} \in \text{span}\{\boldsymbol{a}(\theta_{k'})\}_{k' \neq k}$. We have $\text{span}\{\boldsymbol{a}(\theta_{k'})\}_{k' \neq k} = \mathbb{C}^N$ in general (and this is the case, in particular, for uniform linear antenna arrays with distinct azimuths as shown in Appendix C). Thus, the matrix $\boldsymbol{R}$ must map the entire space $\mathbb{C}^N$ into the orthogonal complement of $\boldsymbol{a}(\theta_k)$. Since this is true for every k, and since $\{\boldsymbol{a}(\theta_k)\}_{k=1}^{K}$ again span $\mathbb{C}^N$ in general, we must have that $\boldsymbol{R} = \boldsymbol{0}$, contradicting the requirement $\text{tr}(\boldsymbol{R}) = 1$. Thus, (7) is infeasible, implying that $K^\star < N + 1$.

APPENDIX C
UNIFORM LINEAR ANTENNA ARRAYS

For a uniform linear antenna array with half-wavelength antenna spacing, we have $a_n(\theta)$ as given by (8). Construct the matrix $\boldsymbol{A} \triangleq \big(\boldsymbol{a}(\theta_k)\big)_{k=1}^{K}$. Note that $\boldsymbol{A}$ is a Vandermonde matrix. Hence, $\text{rank}(\boldsymbol{A}) = \min\{N, K\}$ if $\{\theta_k\}_{k=1}^{K}$ are distinct.

REFERENCES

[1] U. Niesen and J. Unnikrishnan, "Association-aware radar beamforming," in *Proc. Asilomar Conf.*, Oct. 2018.

[2] J. Li and P. Stoica, *MIMO Radar Signal Processing*. Wiley-IEEE Press, 2009.

[3] M. A. Richards, *Fundamentals of Radar Signal Processing*. McGraw-Hill, second ed., 2014.

[4] Y. Bar-Shalom, *Multitarget-multisensor tracking: Advanced applications*. Artech House, 1990.

[5] X. R. Li and V. P. Jilkov, "Survey of maneuvering target tracking. Part I. Dynamic models," *IEEE Trans. Aerosp. Electron. Syst.*, vol. 39, pp. 1333–1364, Oct 2003.

[6] L. Yu, Y. Wei, and W. Ji, "Wide transmit beamforming for the subarrays in MIMO radar," in *Proc. CIE RADAR*, pp. 1–4, Oct 2016.

[7] D. R. Fuhrmann and G. S. Antonio, "Transmit beamforming for MIMO radar systems using signal cross-correlation," *IEEE Trans. Aerosp. Electron. Syst.*, vol. 44, pp. 171–186, Jan. 2008.

[8] B. Friedlander, "On transmit beamforming for MIMO radar," *IEEE Trans. Aerosp. Electron. Syst.*, vol. 48, pp. 3376–3388, Oct. 2012.

[9] J. Lipor, S. Ahmed, and M. S. Alouini, "Fourier-based transmit beampattern design using MIMO radar," *IEEE Trans. Signal Process.*, vol. 62, pp. 2226–2235, May 2014.

[10] D. R. Fuhrmann, J. P. Browning, and M. Rangaswamy, "Signaling strategies for the hybrid MIMO phased-array radar," *IEEE J. Sel. Topics Signal Process.*, vol. 4, pp. 66–78, Feb. 2010.

[11] Y. Li, S. A. Vorobyov, and V. Koivunen, "Ambiguity function of the transmit beamspace-based MIMO radar," *IEEE Trans. Signal Process.*, vol. 63, pp. 4445–4457, Sept. 2015.

[12] A. Hassanien and S. A. Vorobyov, "Transmit energy focusing for DOA estimation in MIMO radar with colocated antennas," *IEEE Trans. Signal Process.*, vol. 59, pp. 2669–2682, June 2011.

[13] A. Khabbazibasmenj, A. Hassanien, S. A. Vorobyov, and M. W. Morency, "Efficient transmit beamspace design for search-free based DOA estimation in MIMO radar," *IEEE Trans. Signal Process.*, vol. 62, pp. 1490–1500, Mar. 2014.

[14] P. Stoica, J. Li, and Y. Xie, "On probing signal design for MIMO radar," *IEEE Trans. Signal Process.*, vol. 55, pp. 4151–4161, Aug. 2007.

[15] W. Zhang and S. A. Vorobyov, "Joint robust transmit/receive adaptive beamforming for MIMO radar using probability-constrained optimization," *IEEE Signal Process. Lett.*, vol. 23, pp. 112–116, Jan. 2016.

[16] J. Bechter, K. Eid, F. Roos, and C. Waldschmidt, "Digital beamforming to mitigate automotive radar interference," in *Proc. IEEE ICMIM*, pp. 1–4, May 2016.

[17] N. Sharaga, J. Tabrikian, and H. Messer, "Optimal cognitive beamforming for target tracking in MIMO radar/sonar," *IEEE J. Sel. Topics Signal Process.*, vol. 9, pp. 1440–1450, Dec 2015.

[18] W. Huleihel, J. Tabrikian, and R. Shavit, "Optimal adaptive waveform design for cognitive MIMO radar," *IEEE Trans. Signal Process.*, vol. 61, pp. 5075–5089, Oct 2013.

[19] Y. Li, W. Moran, S. P. Sira, A. Papandreou-Suppappola, and D. Morrell, "Adaptive waveform design in rapidly-varying radar scenes," in *Proc. IEEE WDD*, pp. 263–267, Feb 2009.

[20] B. Friedlander, "Adaptive waveform design for a multi-antenna radar system," in *Proc. Asilomar Conf.*, pp. 735–739, Oct 2006.

[21] B. Friedlander, "On data-adaptive waveform design for MIMO radar," in *Proc. Asilomar Conf.*, pp. 187–191, Nov 2007.

[22] A. Leshem, O. Naparstek, and A. Nehorai, "Information theoretic radar waveform design for multiple targets," in *Proc. IEEE WDD*, pp. 362–366, June 2007.

[23] J. Tabrikian, "Adaptive waveform design for target enumeration in cognitive radar," in *Proc. IEEE CAMSAP*, pp. 69–72, Dec 2013.

[24] S. Boyd and L. Vandenberghe, *Convex Optimization*. Cambridge University Press, 2004.

[25] S. Boucheron, G. Lugosi, and P. Massart, *Concentration Inequalities*. Oxford University Press, 2013.